The Driftcam: A Buoyancy Controlled Pelagic Camera Trap

Eric J. Berkenpas, Bradley S. Henning, Charles M. Shepard, and Alan J. Turchik
Missions Programs
National Geographic Society
Washington, D.C., United States

***Abstract*—The midwater column of the ocean has been largely unexplored by man. These are regions below the sun-lit upper ocean and above the seafloor. According to the Monterrey Aquarium 2004 Annual Report the midwater column contains the largest communities of species in the world. Despite this, very little is known about the biodiversity in this region of the water column [1]. Little imagery of these species in their natural environment exists.**

An autonomous, deep-submergence, buoyancy-compensated 'Driftcam' has been developed to probe the mesopelagic and bathypelagic regions of the water column. The system utilizes an HD video camera and a 7200 lm LED lighting system inside a polished borosilicate spherical pressure housing. An embedded computer controls the camera and lighting. An electrically driven, hydraulic buoyancy engine has been developed to facilitate depth control through the water column. The buoyancy engine utilizes an encoder-less, stepper-motor driven, hydraulic piston to pump inert oil to and from an external bladder. A pressure transducer provides depth feedback to an embedded, intelligent motor drive. The Driftcam is designed for a controlled operating depth of up to 1500 m and a recoverable depth of 6000 m. Surface recovery is facilitated by a light beacon, a VHF beacon, and an ARGOS satellite transmitter capable of functioning for 1 year. In addition, the system is highly portable, measuring 1.5 m in total length. To date, the system has been deployed over 8 times to depths beyond 100 meters.

***Keywords*—Lagrangian; Floats; AUV; Pelagic; Camera**

I. INTRODUCTION

The midwater column contains the largest communities of species in the world. Very little imagery of these life forms captured in their natural environment exists [1]. Wildlife camera trap technology exists and has been employed on land very effectively to image elusive species. Underwater camera systems have been employed at shallow depths. So-called 'lander' systems have been used to image the extreme deep [2, 3]. Undersea imaging technologies for capturing sea-life in the mid-water column beyond SCUBA diving depth (>70m) typically utilize Manned Submersibles [4], remotely operated vehicles (ROVs), and autonomous underwater vehicles (AUVs) [5].

The so-called Lagrangian floats utilize buoyancy control by adjusting their densities to maintain depth and drift with ocean currents. They have the advantage of requiring no tether and requisite support ship. These systems have been employed to measure deep ocean conductivity, temperature, and depth (CTD) [6, 7]. Recently a Lagrangian float has been employed as a benthic imager [8]. By combining the Lagrangian float with a camera system, lighting and suitable triggering sensors, an undersea camera trap can be created that could capture imagery of pelagic species in-situ.

An inexpensive, autonomous, deep-submergence, tetherless, buoyancy compensated camera trap called the 'Driftcam' has been developed to probe the mesopelagic and bathypelagic regions of the water column.

II. SYSTEM DESIGN

The Driftcam was designed to meet the basic requirements of an underwater camera trap to image elusive pelagic species. The Driftcam must control its buoyancy to a depth of 1500m and must be recoverable from a depth of 6000m. The system must be able to achieve 10 pre-programmed depths and return to the surface via buoyancy control 7 days later. The Driftcam must record high-definition with on-board illumination. Lastly, system must be locatable for 1 year while on the surface via satellite tracking.

A. Dynamic Modeling

In order to achieve these goals, a transient model of the forces acting on the system was created. These forces are illustrated in Fig. 1. In the model, the aggregate force on the Driftcam can be described as a sum of gravity (F_g), buoyancy (F_b), drag (F_d), and a correction force applied by a buoyancy engine (F_{bc}). The force of gravity is described as

$$F_g = m\alpha_g \tag{1}$$

where *m* is the mass the system and α_g is the acceleration due to gravity. Buoyancy is described as

$$F_b = \rho_{sea} V_{disp} \alpha_g \tag{2}$$

where ρ_{sea} is the density of seawater and V_{disp} is the volume displaced by the Driftcam. Drag is approximated by

$$F_d = -sgn(v_f)\frac{1}{2}\rho_{sea} A C_d v_f^2 \tag{3}$$

where v_f is the flow velocity of seawater over the system, A is the cross-sectional area of the Driftcam in the flow, and

C_d is the coefficient of the drag. The velocity of the system in the water column can then be given as

$$v = v_i + \frac{F_g + F_b + F_d + F_{bc}}{m} dt \quad (4)$$

where v_i is the initial velocity of the system and t is time. Depth was calculated by the integration of velocity over time.

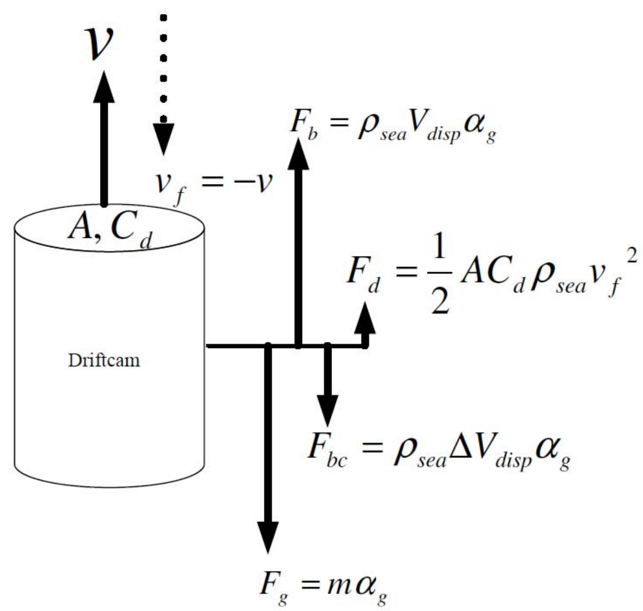

Fig. 1. A diagram of the forces acting on the Driftcam used to model the buoyancy engine and test the control system algorithm.

The transient model was implemented in MATLAB (MathWorks) and used to estimate the energy requirements of the system, the size and precision of the buoyancy engine, and the required precision and accuracy of the depth sensor. The model also aided in the design and tuning of the buoyancy control algorithm.

B. Instrument Layout

The physical layout of the Driftcam system is shown in Fig. 2. The top of the system consists of a 43cm diameter, 2.1cm thick borosilicate glass sphere (Nautilus Marine Service, GmbH). The sphere is rated to a depth of 12,000m. The top hemisphere contains satellite and VHF radio beacons. It also holds lighting which projects out of the sphere to mirrored reflector arms mounted by an external ring assembly. The reflector arms serve to separate the light source from the camera. The bottom hemisphere is polished and contains an HD video camera. The camera controller and batteries are also contained in the sphere. The sphere is mostly empty volume and thus serves as floatation for the system.

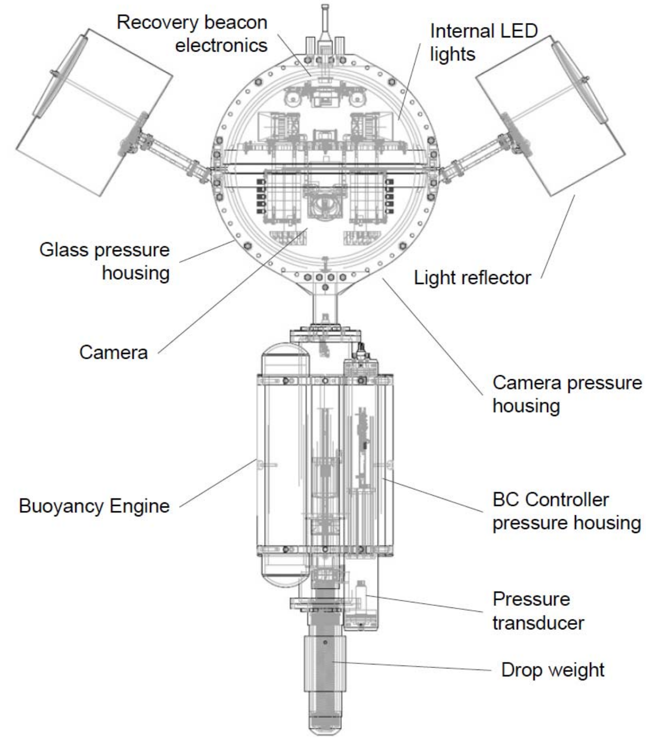

Fig. 2. Shown is the Driftcam mechanical layout. The camera module, a polished glass sphere at the top houses the video camera, lighting, and camera control electronics. The buoyancy compensator provides vertical locomotion within the water column. A backup drop-weight hangs at the bottom and provides 9 kg of additional buoyancy in the event of a fault.

Mounted beneath the glass sphere is an automatic buoyancy engine or buoyancy compensator (BC) containing a piston, batteries, a depth sensor, and an embedded controller, which serves to adjust the buoyancy of the Driftcam system. This allows vertical locomotion within the water column. In addition to the buoyancy generated by the sphere, syntactic floatation is mounted to the buoyancy engine to trim the system buoyancy to 0N.

At the bottom is a 9 kg steel drop-weight, which is released by the system as a failsafe should the buoyancy engine fail. The drop-weight is released by the Camera Controller through the use of a burn-wire. Additionally, a galvanic timed release (Neptune Marine Supply) is used as a secondary failsafe to release the drop-weight.

C. Buoyancy Engine

A single stroke hydraulic pump was built to provide the necessary system density change for vertical locomotion. The system uses an electric drive made up of commercially available components. A stepper motor (24Y506S-LW8, Anaheim Automation) is coupled to a 40:1 planetary gear box (Anaheim Automation) which provides 35Nm of torque to drive a 40mm diameter, 5mm pitch steel ball screw to provide lateral motion on a sealed brass piston. The drive was designed to allow the piston to actuate against 15MPa of differential pressure. An electromechanical brake (Inertial Dynamics) provides necessary stopping force when the motor is not energized. The piston pumps mineral oil (Marcol 52, ExxonMobil) into an external bladder which acts as the expandable volume.

The Driftcam's buoyancy engine was modeled after similar previously developed single-stroke Lagrangian float engines [6, 7, 8] with one notable difference (Fig. 3.). Typical engines pump oil directly into an external bladder while their electric drives remain dry and at about 1 atm. The Driftcam's buoyancy engine operates with oil on the reverse side of the piston, pulling a partial vacuum on the cylinder. The electric drive operates at ambient pressure immersed in oil. Reversing the oil has the advantage of allowing the ball screw to operate in tension rather than compression taking advantage of its material properties. Additionally, the pressure housing can be reduced to cover only the piston cylinder as the drive now operates at ambient pressure and requires no pressure tolerant casing. The oil also serves to lubricate and cool the drive during operation. Lastly, the system is more leak-tolerant since any oil that has leaked past the piston seal can be discharged out of the cylinder via a one-way valve. These advantages come at the cost of reduced overall buoyancy compared to the empty volume around the drives used by typical buoyancy engines.

The buoyancy of the entire Driftcam system was calculated over its operating depth of 0-1500m and expected range of ocean salinity and temperature over this depth range. The operational envelope at a salinity of 35g/kg is shown in Fig. 4. This graph indicates the system's depth will be controllable by the buoyancy engine within its operating depth range. Material constants for seawater and Driftcam system components were obtained from [9, 10].

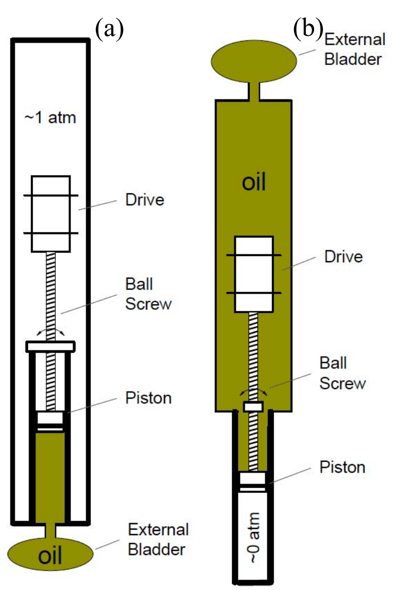

Fig. 3. (a) Illustrated on the left is a typical single stroke buoyancy engine. Oil is pumped directly into a bladder and the drive system remains at around 1 atm. (b) On the right, is the configuration chosen for the Driftcam. The piston pulls a partial vacuum and the drive operates at ambient pressure in oil (b).

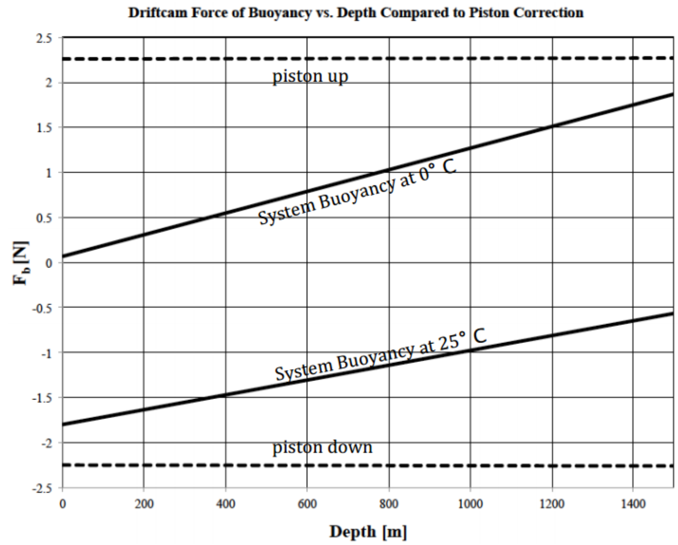

Fig. 4. The operational envelope of the Driftcam at a salinity of 35 g/kg (at 0 and 25 °C). The Driftcam's buoyancy increases with an increase in depth (solid lines). This is less than the buoyancy adjustment afforded by the buoyancy engine (dashed lines).

D. Electrical Design

The Driftcam contains three separate electronic systems (Fig. 5) that operate independently from one another: the recovery beacon, the camera controller, and the BC controller.

The beacon consists of a 403MHz Argos satellite transmitter for global tracking, and a 150MHz VHF radio transmitter for short-range tracking during recovery operations. The Argos system transmits once every 90s, while the VHF transmits once per second. The beacon is powered by a 3.6V 51Ahr $LiSOCl_2$ primary battery pack. The beacon is energized by a magnet switch before the Driftcam is deployed. Beacon battery life is estimated at 1yr.

The camera controller consists of a custom-designed PCB based on the Microchip Technology PIC24HJ256GP610A (PIC24) microcontroller. The camera controller interfaces with the HD video camera (HDR-XR520V, Sony) via a Sony LANC connection. The camera captures video in 1080i format at 60 frames per second and records to an internal 240 GB hard drive. For lighting, two high-output solid-state LEDs (BXRA-C4500, Bridgelux) provide a nominal 7200 lumens total. To release the drop-weight, a power MOSFET switch delivers current directly from the main battery to a single-use burn wire. When energized, the wire disintegrates at an exposed metal point and releases the drop weight, allowing the Driftcam to ascend should the buoyancy engine fail. The camera controller is powered by an 11.1V 52Ah lithium-polymer battery pack. This allows 6hrs of continuous video with lighting. Two waterproof bulkheads (BH10MTi, SubConn) provide an external electrical connection to allow data transfer and battery charging.

The BC controller is also made up of a custom-designed PCB based around the PIC24 microcontroller, as well as an energy efficient, high current, high precision microstepping driver for bipolar stepper motors. The PIC24 sends the driver step pulses and a direction signal, and the driver intelligently uses these signals to deliver motor current by switching power MOSFET bridges. Depth measurement is provided by a diaphragm pressure transducer mounted to the BC Controller pressure housing (Series 3L, Keller). The pressure transducer signal is sampled by a 10-bit analog to digital (AD) converter on the PIC24. The BC Controller is powered by a 22.2V 3.7Ah lithium-polymer battery pack. This allows 5hrs of continuous piston actuation. A waterproof bulkhead (IE55, Teledyne Impulse) facilitates programming and battery charging. As with the recovery beacon and camera controller, the BC controller is switched on and off via a magnet switch.

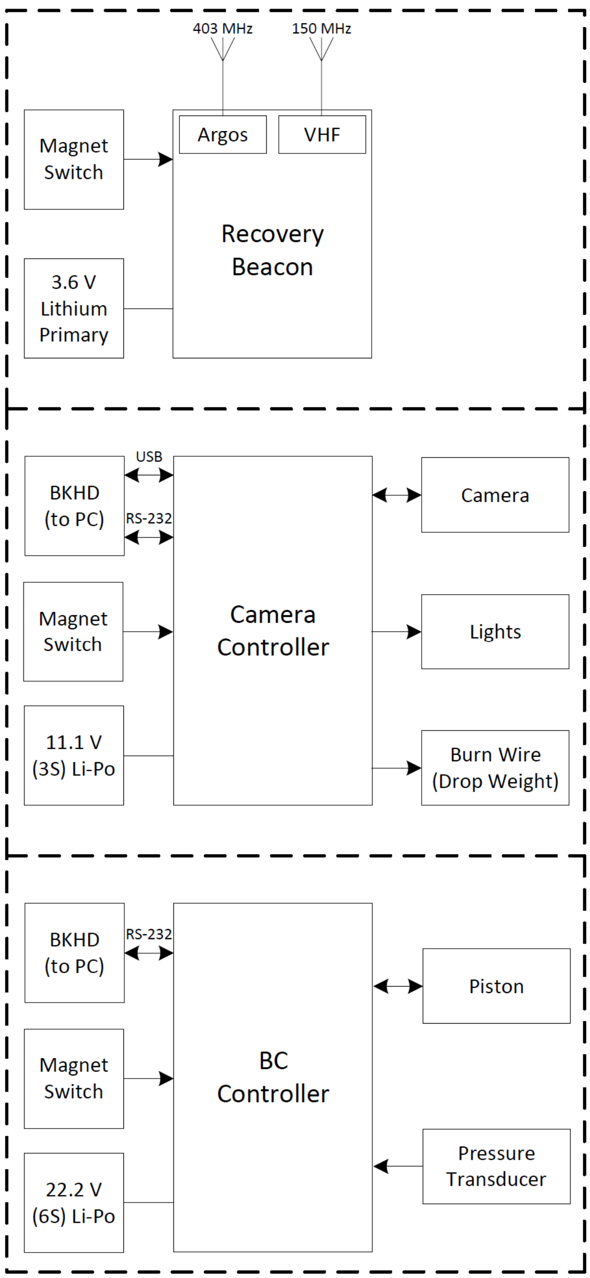

Fig. 5. A block diagram of the Driftcam system. The recovery beacon, camera controller, and buoyancy engine are completely isolated.

E. Firmware

Firmware was created for both the Camera Controller and the BC Controller as two separate queued finite state machines (FSM). The FSM was chosen since it allowed designers to develop controller algorithms which could carry out relatively complex tasks while maintaining rigid, deterministic system behavior [11]. Entry point occurs on system boot and exit occurs when all tasks are complete. The state machine used to control the buoyancy engine is shown in Fig. 6. Decision states (e.g. Check for End of Mission) are queued and then queue task states based on system inputs (Battery Level, Depth etc). Task states (e.g. Measure Depth) are then executed sequentially until another decision state is executed. The FSMs were implemented for the PIC24 in C using the XC16 Compiler (Microchip Technology).

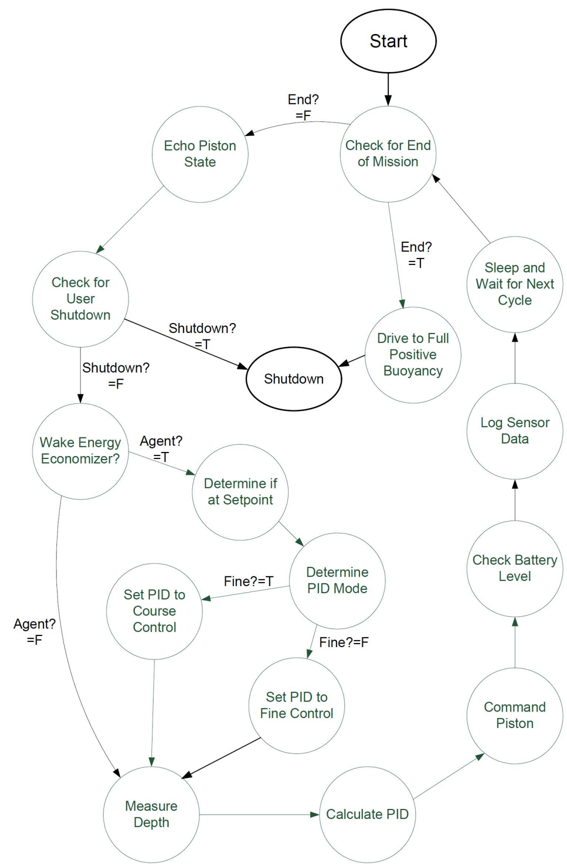

Fig. 6. Buoyancy engine control firmware is implemented as a state machine. Decision states queue task states based on system inputs, which are de-queued and executed in sequence.

The depth control algorithm was developed in MATLAB and tested with the transient numerical model before being ported to C for the BC Controller. The algorithm utilizes a cascaded PID-PI control loop operating at a frequency of 1 Hz (Fig. 7). The outside PID loop endeavors to minimize error between the pre-programmed depth set-point and the measured depth by adjusting the piston position and therefore the buoyancy. The inside PI loop maintains the position set-point by minimizing the error between the commanded piston position and the estimated position.

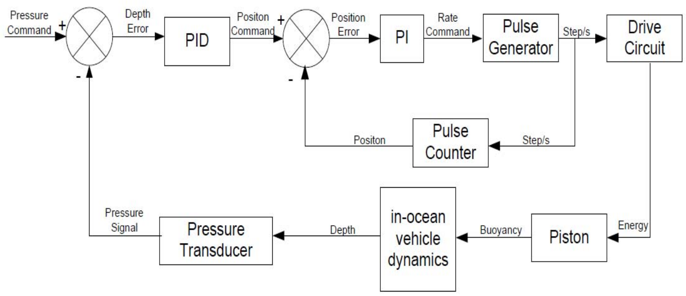

Figure 7: Shown is a block diagram of the cascaded PID-PD control system used to control the buoyancy engine of the Driftcam.

III. TESTING

Driftcam system testing was carried out to evaluate system performance compared to design goals as well as validate the transient model. System testing was performed in two phases; tuning and sea-trials.

To reduce the time and cost to tune the system, the transient model was utilized to determine optimal PID control parameters. In order to correct transient model parameters and validate PID parameters, pool testing was carried out in a 7.5m deep 1.4 ML freshwater pool at the Space Systems Laboratory at the University of Maryland. These tests were carried as a series of 10min and 30min 'missions' to a depth of 2.5m. Telemetry from the Driftcam was relayed in real-time to a topside computer via a 10m RS-232 tether.

Sea-trials were used to test the camera system, buoyancy engine, recovery beacons, and the backup drop-weight in actual sea conditions. Sea-trials were performed during a National Geographic expedition to the Desventuradas Islands in February of 2013. During sea-trials, the Driftcam was deployed 8 times untethered. Because of weather conditions and strong currents, sea-trial tests were limited to 3 hours and a maximum depth of 200 m. Video and BC control data was stored in non-volatile memory within the Driftcam system during each sea-trial and downloaded after each recovery.

IV. RESULTS

Pool testing resulted in good agreement between the transient model and in-water system performance. This allowed PID parameters to be selected which allowed the system to maintain controlled depth within 1m of the set-point. Pool testing also indicated a large amount of noise on the derivative signal which made this control parameter impractical for control. Testing did confirm that PI-PI was sufficient for effective depth control of the buoyancy compensator system. These control parameters were used during sea-trials.

A typical depth profile is shown in Fig. 8. During this test, the Driftcam was sent to 2 depths; initially 145m, and then 0m at 60min. The actual depth is shown as a solid line and indicates the systems achieving depth set-point at about 30min. The dashed line shows the transient model for comparison. Disagreement between the transient model and the sea-trial depths between 80min and 120min is most likely due to temperature dependence of the pressure transducer when it was exposed to cooler waters at depth. This pressure transducer temperature dependence was not implemented in the transient model.

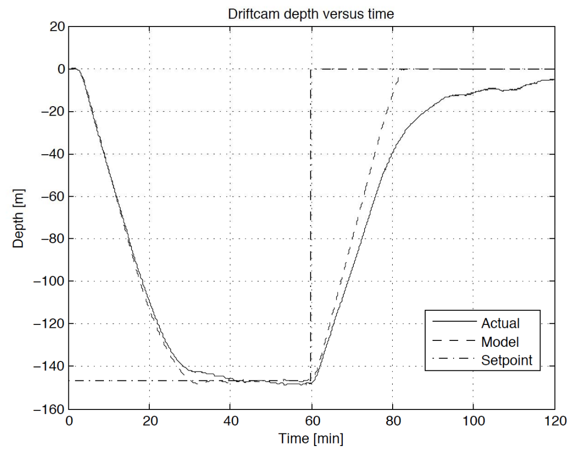

Fig. 8. This curve shows a Driftcam sea-trial test to 145m depth compared to a numerical simulation.

A photograph of the Driftcam in operation at a depth of 20m is shown in Fig. 9a. Video of several species of fish was obtained during sea-trials. Fig. 9b shows a frame taken from video of 'Amberjacks' (Seriolas) at a depth of 40m.

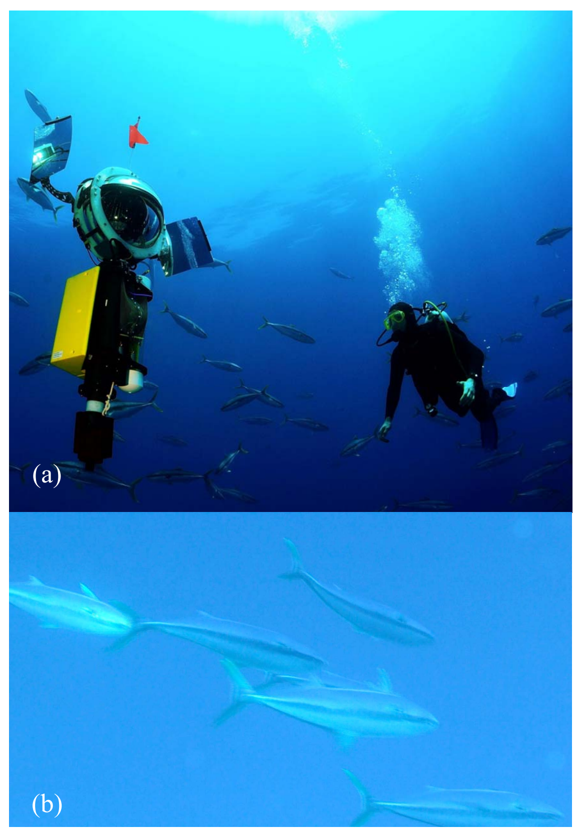

Fig. 9. (a) A diver observes the operation of the Driftcam during sea-trials near the Desventuradas Islands, Chile. (b) A video-frame from the Driftcam's camera system showing 'Amberjacks' at a depth of 40m.

V. SUMMARY

The basic building blocks of a tetherless, free-floating pelagic camera trap have been developed and tested at sea. A camera system has been created which takes high quality HD video of pelagic species.

Currently the camera system is triggered by pre-programmed time and not the presence of pelagic species. This limits the amount of sea-life captured in the limited on-board memory. Future work will involve the creation of a motion trigger to allow the system to automatically capture video of species when they are detected.

A buoyancy engine, control system, and a practical dynamic numerical model of the Driftcam system have been developed. A combination of numerical simulation and pool testing has proven to be an effective method for tuning the control system algorithm. Pool testing indicated shortcomings in the resolution and signal to noise ratios of the pressure transducer and its effect on the derivative control parameter. Although the derivative signal is not necessary for control, it caused the system to take much longer to achieve its depth set-point compared to PID-PI reducing battery life. Future work will involve improving the resolution, accuracy, and signal-to-noise ratio of the pressure transducer to allow for a more accurate derivative estimation.

The full Driftcam system has been tested 8 times in the field showing the proper function of the recovery beacon, camera and lighting system, buoyancy engine, and backup drop-weight. This testing has proven the efficacy of the Driftcam system as an effective pelagic camera trap.

ACKNOWLEDGEMENTS

This work has been funded by the National Geographic Society, as well as the generous support of Joanie Nasher. The authors would like to thank Dr. David Akin of the University of Maryland's Space Systems Laboratory, which provided excellent facilities for pool testing. Dr. Enric Sala, head scientist, generously allowed sea-trials testing of the Driftcam system on the National Geographic Pristine Seas Expedition to the Desventuradas Islands.

REFERENCES

[1] M. McNutt et al., "MBARI 2004 Annual Report," MBARI, Moss Landing, CA, Annual Report, pp. 19-21, 2004.

[2] K. Hardy, M. Olsson, A. Yayanos, J. Prsha, W. Hagey, "Deep Ocean Visualization Experimenter (DOVE): Low-Cost 10km Camera and Instrument Plaform," Proceedings of the MTS/IEEE Oceans '02 Conference, v4, pp 2390-2394, 2002.

[3] I. Priede, P. Bagley, S. Way, P. Herring, J., Partridge, "Bioluminescence in the deep sea: free-fall lander observations in the Atlantic Ocean off Cape Verde," Deep Sea Research, i53, pp 1272-1283, 2006.

[4] H. A. Arnold, "Manned Submersibles for Research," American Association for the Advancement of Science, v158, n3797, pp 84-90, 1968.

[5] M. Woolsey, V., Asper, A., Diercks, K. McLetchie, "Enhancing NIUST's SeaBED Class AUV, Mola Mola," Autonomous Underwater Vehicals (AUV), 2010 IEEE/OES, pp. 1-5, Sept. 2010.

[6] J. Gould, "From Swallow floats to Argo-the development of neutrally buoyant floats," Deep-Sea Research II, v52, pp 529-543, 2005.

[7] R. Davis, J. Sherman, J. Dufour, "Profiling ALACEs and Other Advances in Autonomous Subsurface Floats," Journal of Atmospheric and Oceanic Technology, v18, pp 982-992, 2000.

[8] C. Roman, G. Inglis, B. McGilvray, "Lagrangian floats as sea floor imaging platforms," Continental Shelf Research, 2011.

[9] E. A. Avallone, T. Baumeister, Marks Standard Handbook for Mechanical engineers, McGraw Hill,1987, pp 6-9, pp3-36, pp3-35

[10] G. Totten, V. Negri, Handbook of hydraulic Fluid Technology, second edition, Taylor and Francis Group, 2012 pp 726

[11] M. Gomez, "Embedded state machine implementation," Embedded Systems Programming, pp. 40-50, Dec. 2000.